Russian Physics Journal, Vol. 55, No. 8, January, 2013 (Russian Original No. 8, August, 2012)

INVESTIGATION OF THE OPTICAL CHARACTERISTICS OF CIRRUS CLOUDS WITH ANOMALOUS BACKSCATTERING

I. V. Samokhvalov, I. D. Bryukhanov, S. V. Nasonov, I. V. Zhivotenyuk, and A. P. Stykon

UDC 535.361; 551.501.776

Data of polarization laser sensing of high-level clouds obtained within the year from April, 2011 are processed. Attention is focused on cirrus clouds with anomalous reflection. The optical thickness and average extinction coefficient of cirrus clouds comprising horizontally oriented crystals are estimated for sensing radiation with different polarization states.

Keywords: cirrus clouds, anomalous backscattering, optical cloud layer thickness, scattering ratio.

Cirrus clouds belong to high-level clouds (HLCs). They are formed at altitudes of 8–12 km, are sufficiently transparent in the visible wavelength range, and have large horizontal extension. As a rule, such clouds consist of crystal particles having different sizes and shapes. The spatial crystal orientation in clouds affects significantly the solar radiation transfer and scattering in the atmosphere; therefore, cirrus clouds are an important climate forming factor. Crystals in cirrus clouds often have strictly horizontal orientation. Such clouds are called *specular* [1], since their backscattering coefficient (for sensing in the *zenith*) is very high.

In the present study, the optical thicknesses of cirrus clouds with anomalous backscattering are presented for radiation with four polarization states, including three linear polarization states and one circular polarization. In addition, an attempt is made to explain under what meteorological conditions clouds with specular reflection are formed. To this end, to analyze the experimental light backscattering matrices (LBSMs), information on the vertical stratification of the pressure, temperature, wind direction and modulus, and other meteorological parameters near the observation point was considered. Investigations were performed with a high-altitude polarization lidar developed at the National Research Tomsk State University (TSU) that allowed the LBSM to be determined [2].

Sensing was carried out in the zenith. A Nd:YAG laser with a working wavelength of 532 nm, pulse repetition frequency of 10 Hz, and energy per pulse of 40 mJ was used as a source of sensing radiation. The Cassegrain telescope with a diameter of the main mirror of 0.5 m and a focal distance of 5 m served as a receiving objective. A field stop 3 mm in diameter specifying the field-of-view angle of the receiving telescope, a positive lens transforming a diverging beam into a quasi-parallel one, an interference filter, and a Wollaston prism at the exit from which two beams were formed with mutually orthogonal polarization states were successively arranged in the receiving channel along the propagation path of scattered radiation. The beam intensities were registered with photoelectron multipliers operating in the photon counting regime. The first registration channel was considered the channel in which radiation linearly polarized in the plane coinciding with the oscillation plane of the electric vector of laser radiation (the reference plane) was registered.

The special feature of the TSU lidar is the presence of identical units that transform the radiation polarization state in the transmitting and receiving channels [2]. Depending on the configuration of elements in these units, sensing radiation had four polarization states characterized by the normalized Stokes vector $\boldsymbol{S}_i$, and the polarization elements in the receiving channel formed the polarimeter with the corresponding set of instrumental vectors $\boldsymbol{G}_j$ (the subscripts i and

National Research Tomsk State University, Tomsk, Russia, e-mail: sam@elefot.tsu.ru. Translated from Izvestiya Vysshikh Uchebnykh Zavedenii, Fizika, No. 8, pp. 63–67, August, 2012. Original article submitted June 15, 2012.

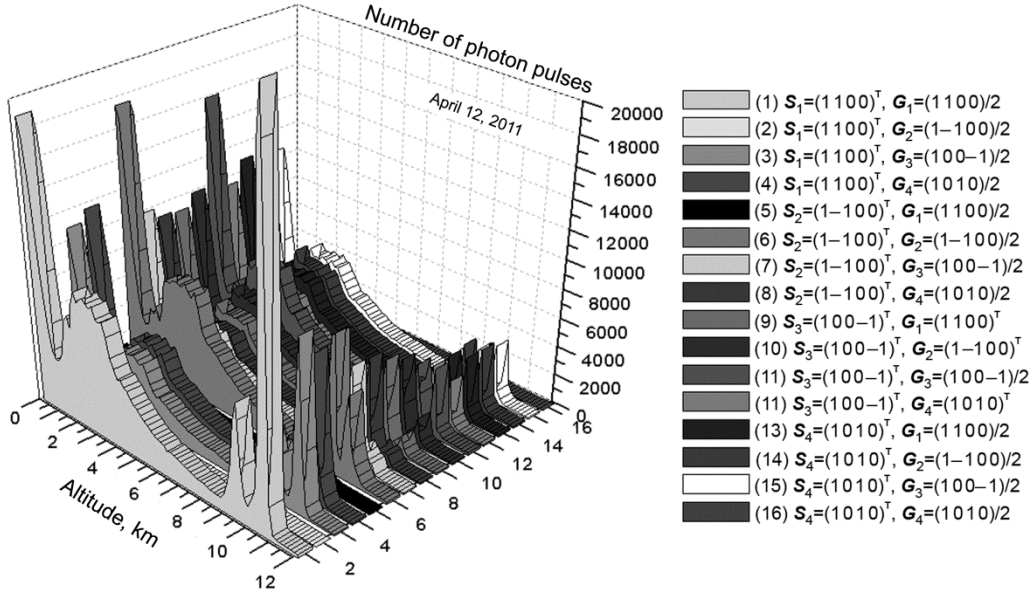

Fig. 1. Vertical profiles of the backscattered radiation intensity (registered on April 12, 2011).

j take values 1, 2, 3, and 4). For four combinations of the Stokes vector of the transmitter and four states of the instrumental vector, 16 backscattered radiation intensities were measured, which allowed 16 elements of the LBSM to be calculated. The time of measuring 16 profiles of the backscattered radiation intensity was 6–14 min (for accumulation of 200–500 laser pulses with frequency of 10 Hz). The lidar operated in the semi-automatic regime controlled by the operator with the help of a computer.

Figure 1 shows an example of the vertical profiles of the backscattered radiation intensity registered on April 12, 2011 (from 21:32 to 21:46, local time).

The measurement run lasted ~14 min, which corresponded to accumulation of 500 laser pulses. The altitude, in kilometers, is plotted on the *x* axis of the figure, and the number of single-electron pulses received from the corresponding altitude and accumulated by the registration system is plotted on the *y* axis. Each vertical profile is explained on the right of the figure, where $\boldsymbol{S}_i$ indicates the polarization state of sensing radiation characterized by the normalized Stokes vector, and $\boldsymbol{G}_j$ indicates the instrumental vector of the receiving lidar system characterizing the joint action of polarization devices in the receiving channel.

To characterize quantitatively the backscattering coefficient at altitude *H* in the atmosphere, the scattering ratio $R(H) = (\beta_\pi^m + \beta_\pi^a)/\beta_\pi^m$ was used representing the ratio of the sum of the aerosol and molecular backscattering coefficients to the molecular backscattering coefficient.

The criterion of *specular reflection* for HLCs has the following characteristics: cloud altitude of 5–12 km, cloud thickness ≤1 km, scattering ratio $R(H) > 10 - 20$, and value of the backscattering matrix element $m_{44} < -0.4$ [3]. The procedure of estimating the optical cloud thickness was based on the application of the laser sensing equation [4].

Figure 2 shows an example of the vertical profile of backscattered signal power *P*(*H*) in one of the receiving lidar channels. The first peak of the signal power P_{NF}^m from the altitude range adjacent to the receiving lidar system is due to multiple scattering in the near field (NF) zone of the lidar: in the altitude range in which the radiation patterns of the receiver and transmitter have not yet been intersected, and singly scattered radiation from the transmitter cannot arrive at the photodetector. Above the near field zone, scattered radiation starts to fall within the field-of-view angle of the receiver, the backscattered signal power increases, reaches a maximum in the clear (background) atmosphere (BGA) P_{BGA}^m, and then decreases according to the laser sensing equation. The second maximum $P_{\max}$ is formed within the cloud. The clear atmosphere is the atmosphere in its natural background state in which radiation scattering is caused mainly by air density fluctuations (molecular scattering), and only a small portion of radiation is scattered by aerosols

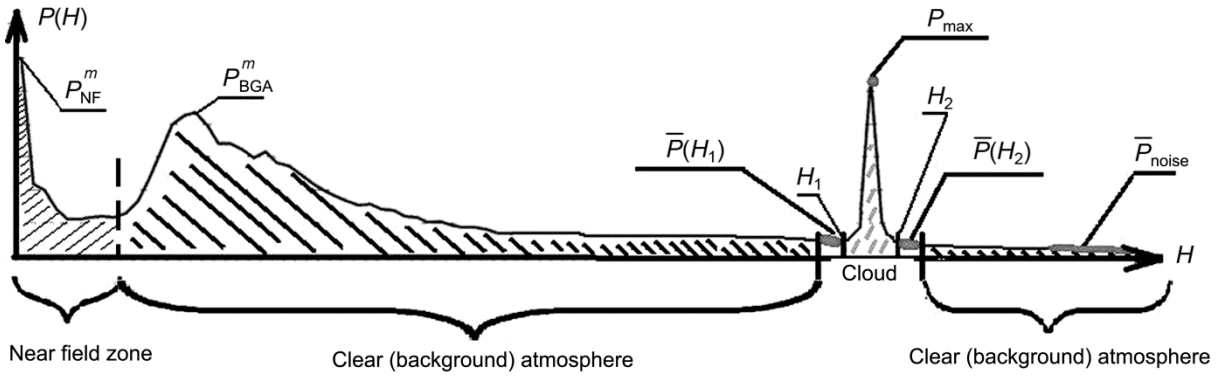

Fig. 2. Typical lidar signal from high-level clouds.

(aerosol or Rayleigh scattering). In Fig. 2, H_1 and H_2 denote altitudes before and after the cloud; they specify the lower and upper cloud boundaries.

Since the maximum signal power P_{max} backscattered from the cloud is high in comparison with the signal from the clear atmosphere before and after the cloud, the scattering ratio can be calculated with sufficient accuracy from the formula $R = P_{max} / \overline{P}_{H_1}$, where $\overline{P}(H_1)$ is the average signal power in the layer under the cloud.

The average lidar signal power $\overline{P}(H_1)$ was calculated from four measurements of $P(H_i)$ at altitudes in the range 150–600 m under the cloud before its lower boundary. The lidar signal power $\overline{P}(H_2)$ was calculated analogously. To take into account the effect of noise due to sky luminescence and the intrinsic noise of the photoelectron multiplier, the average noise power $\overline{P}_{noise}$ was estimated for each realization $P(H)$. The component $\overline{P}_{noise}$ was estimated for altitudes from which the lidar signal was negligibly small compared to noise. This corresponded to the time interval exceeding 150 μs after the moment of sensing pulse transmission.

The optical cloud thickness was calculated from the laser sensing equation written for one of the polarization states of sensing radiation. Having estimated signal powers received from altitudes before and after the cloud $\overline{P}(H_1)$ and $\overline{P}(H_2)$, we calculated their ratio, the logarithm of which determined the optical cloud thickness:

$$\tau(\Delta h) = \int_{H_1}^{H_2} \alpha(z)dz = \frac{1}{2}\ln\frac{P(H_1)}{P(H_2)}\frac{\sigma_\pi(H_2)H_1^2}{\sigma_\pi(H_1)H_2^2}. \quad (1)$$

Here $\sigma_\pi(H_2)$ and $\sigma_\pi(H_1)$ are the backscattering coefficients for the clear atmosphere, and α is the extinction coefficient. In the first approximation, the ratio of the coefficients $\sigma_\pi(H_2)$ and $\sigma_\pi(H_1)$ can be set equal to 1 for the clear atmosphere if the difference between the altitudes H_1 and H_2 is small: $(H_2 - H_1) \le 500$ m. Otherwise, the ratio can be estimated for the standard atmosphere or from experimental data on sensing of the clear (background) atmosphere (without clouds).

There were about 60 days favorable for HLC sensing in 2011, namely, days without high and medium level clouds. Since April till December 2011, 15 cases of observations of specular reflecting layers in HLC were registered.

Results of eight sensing runs are presented in Table 1. The date of sensing is indicated in the first column of the table, the average altitude H_1 of the lower cloud boundary observed in the experiment is given in the second column, the average geometrical thickness ΔH of the cloud layer is given in the third column, the average optical thickness of the cloud layer and its minimum and maximum values are given in the fourth column, the minimum and maximum scattering ratios $R(H)$ registered in the cloud layer during the sensing run are presented in the fifth column, the polarization degree p determined as $p = (\sqrt{Q^2 + U^2 + V^2})/I$, where I, Q, U, and V are the Stokes parameters of the

TABLE 1. Characteristics of Specular Reflecting Layers in Cirrus Clouds

Date	Average LCB altitude H_1, km	Average thickness ΔH, m	Optical thickness: average; min–max	Scattering ratio $R(H)$	Polarization degree p	$-m_{44}$ of the LBSM	Meteorological data at altitudes of observations of specular reflecting layers		
							Temperature, °C: Novosibirsk Kolpashevo	Dew point, °C: Novosibirsk Kolpashevo	Relative humidity, % Novosibirsk Kolpashevo
1	2	3	4	5	6	7	8	9	10
April 11, 2011	9.15	600	0.18; 0.08–0.31	2.6 13.8	0.96 0.98	0.79 0.92	–52* –57**	–56 –63	50 ↑ 51 ↑
April 19, 2011	10.6	450	0.22; 0.14–0.3	1.4 21.2	0.98 0.99	0.57 0.60	–64 (–66) –63 (–65)	–73 (–69) –70 (–68)	30 ↑ (67) 38 ↑ (72)
May 30, 2011	11.1	600	0.22; 0.12–0.39	3.0 43.4	0.96 0.99	0.63 0.85	–54 –55	–59 –60	56 54
June 7, 2011	11.4	450	0.21; 0.05–0.44	6.8 15.2	0.97 0.98	0.70	–56 –56	–62 –	47 –
September 26, 2011	6.4	2200	0.72; 0.16–1.39	2.5 39.1	0.96 0.99	0.67 0.88	–29 (–24) –30 (–28)	–37 (–28) –31 (–37)	46 (78) 96 (44)
September 27, 2011	11.5	600	0.39; 0.14–0.58	2.5 194.3	0.97 0.99	0.73 0.91	–61 –63	–69 –69	34 44
October 17, 2011	8.2	1500	0.52; 0.18–1.11	39.6 88.6	0.92 0.99	0.89 0.92	–46 –50	–52 –55	54 59
December 1, 2011	3.6 and 5.5	450	0.30; 0.12–0.72	2.0 142.2	0.98 0.99	0.53 0.77	–32 –39	–37 –45	61 ↓ 56 ↑

*Novosibirsk; **Kolpashevo.

lidar signal received from the cloud, is indicated in the sixth column, and the element $-m_{44}$ (with the minus sign) of the normalized LBSM that characterizes the degree of horizontal orientation of crystal particles is given in the seventh column [3]. The meteorological data registered at two closely situated stations in Novosibirsk (~250 km to the southwest of the experimental site) and Kolpashevo (~240 km to the north of the observation site) and taken from the site of Wyoming University (USA) [5] are given in the last three columns.

An analysis of the results obtained demonstrated that the altitude of the HLC comprising oriented ensembles of crystal particles changes in wide limits; its seasonal variations are clearly traced, namely, the average altitudes of cirrus clouds over Tomsk (56.48°N, 85.05°E) are 7.7 km in winter and 9.9 km in summer. The cloud thickness above the observation site changes significantly depending on the synoptic conditions. However, its annual variations are insignificant, and its average value is about 0.5–0.8 km. Moreover, the observed clouds sometimes are differently distributed along the vertical direction dividing into separate layers of various thicknesses separated by the cloudless atmosphere. The relative humidity at altitudes of 9–10 km is 52–53%, and the difference between the air temperature and the dew point is about 5°. The situation with the temperature and humidity is close to saturation for ice.

Table 2 gives the results of successive sensing events of a cirrus cloud by radiation with four polarization states every few minutes. From the table it can be seen that the optical cloud thickness during measurements changed not only when going from one polarization state of sensing radiation to another, but also with time for the same polarization state during 2–5 min. The scattering ratio changed from 3 at 22:30 to 194 at 20:47, which testified to significant temporal fluctuations of the preferred orientation of crystal particles. The characteristic time of change of the particle orientation is less than a minute.

This work was partly supported by the Ministry of Education and Science of the Russian Federation under Federal Special Program “Research and Development of Priority Directions of the Development of Scientific and Technological Complex of Russia for 2007–2013” (State Contracts Nos. 16.518.11.7048 and 14.518.11.7053), the

TABLE 2. Sensing on September 27, 2011 for Cloud Altitude of ≈11 km, Cloud Thickness of ≈600 m, and $m_{44} = -(0.73–0.91)$

Linear horizontal polarization					
Local time	20:40	20:47	21:10	22:21	22:30
Optical thickness	0.31	0.14	0.31	0.44	0.55
Scattering ratio	24	194	10	14	3
Linear vertical polarization					
Local time	20:42	20:49	21:14	22:23	22:34
Optical thickness	0.26	0.23	0.41	0.51	0.42
Scattering ratio	41	146	5	13	4
Circular polarization					
Local time	20:44	20:51	21:18	22:25	22:38
Optical thickness	0.26	0.24	0.37	0.49	0.44
Scattering ratio	50	123	3	3	4
Linear polarization at 45°					
Local time	20:46	20:53	21:22	22:27	22:43
Optical thickness	0.58	0.5	Non-specular	0.4	0.41
Scattering ratio	94	10	Non-specular	4	4

Federal Special Program “Scientific and Pedagogical Personnel of Innovative Russia” for 2009–2013 (State Contract No. 14.740.11.1145), and the Russian Foundation for Basic Research (grant No. 11-05-01200a).

REFERENCES

1. C. M. R. Platt, J. Appl. Meteorol., No. 17, 1220–1224 (1978).
2. I. V. Samokhvalov, B. V. Kaul’, S. V. Nasonov, *et al*., Opt. Atm. Okeana, **25**, No. 5, 403–411 (2011).
3. B. V. Kaul’, I. V. Samokhvalov, and S. N. Volkov, Appl. Opt., **43**, No. 36, 6620–6628 (2004).
4. V. E. Zuev, B. V. Kaul’, I. V. Samokhvalov, *et al*., Laser Sensing of Industrial Aerosols [in Russian], Nauka, Novosibirsk (1986).
5. http://weather.uwyo.edu/upperair/sensing.html.